

SOME RESEARCH RESULTS OF BASIC PHYSICS OF SINGLE ELECTRON TRANSISTOR

MỘT SỐ KẾT QUẢ VẬT LÝ CƠ BẢN CỦA TRANSISTOR ĐƠN ĐIỆN TỬ

Lê Hoàng Minh¹, Đinh Sỹ Hiền²

¹Ho Chi Minh City University of Technology and Education

²Ho Chi Minh City University of Science

Received 22/12/2016, Peer reviewed 04/01/2017, Accepted for publication 10/02/2017

ABSTRACT

Single electron transistor (SET) is a key element in current research area of nanoelectronics and nanotechnology, which can offer nano-feature size, low power consumption and high operating speed. SET is a new nanoscale switching device; it can control the motion of the single electron. The goal of this paper is to discuss about the basic physics of the SET and focuses on simulation of basic quantum device characteristics like tunneling effect, Coulomb blockage, Quantum dot, Coulomb staircase and Coulomb oscillation. The current-voltage characteristics of SET are explored for illustration.

Keywords: *Single electron transistor, Current-voltage characteristics, Coulomb blockage, Coulomb staircase, Coulomb oscillation.*

TÓM TẮT

Transistor đơn điện tử (SET) là một yếu tố cơ bản trong lĩnh vực nghiên cứu về điện tử nano và công nghệ nano hiện nay. SET cho kích thước đặc tính nano, tiêu tốn công suất thấp và tốc độ làm việc cao. SET là một linh kiện chuyển mạch thang nano mới; có thể điều khiển chuyển động của một điện tử. Mục tiêu của bài báo này là bàn về vật lý cơ bản của SET và tập trung lên mô phỏng đặc trưng lượng tử cơ bản của linh kiện như hiệu ứng xuyên hầm, khóa Coulomb, chướng lượng tử, bậc thang Coulomb và dao động Coulomb. Những đặc trưng dòng-thế được nghiên cứu kỹ dùng để minh họa.

Từ khóa: *Transistor đơn điện tử, đặc trưng dòng-thế, khóa Coulomb, bậc thang Coulomb, dao động Coulomb.*

1. INTRODUCTION

Rapid progress in microelectronics has pushed the MOSFET dimension toward the physical limit (10 nm). In the future it is probable that the nano-MOSFETs could be replaced by new fundamental devices like single electron transistor (SET). SETs have attracted much attention for IC applications because of their nano-feature size, ultra-low power dissipation, high frequency, new

functionalities, and CMOS compatible fabrication process [1].

After their discovery in the 1986 [2, 3], there has been extensive research on fabrication, design and modeling of SETs [4]. SETs with a variety of structures were proposed and fabricated by using different methods [5-7]. SETs have been fabricated to operate at room temperature [8-10].

Molecular quantum dot [11] can display SET's behavior. 1D structures, such as carbon nanotubes and nanowires, can act as SETs [7]. Recent advances in grapheme [12] show promise for SETs.

Research on SET modeling and simulation has been an active area. Monte Carlo simulation has been widely used to model SETs. SIMON [13] and MOSES [14] are the two most popular SET simulators. Uchida *et al.* proposed an analytical SET model and incorporated it into SPICE [15]. Inokawa *et al.* extended this model to a more general form to include asymmetric SETs [16]. Mahapatra *et al.* proposed a simulation framework for hybrid SET/CMOS circuit design and analysis [17]. In contrast, model used non-equilibrium Green's function method (NEGF) [18] commonly used in the nanoscale devices and are superior in terms of simplicity.

In this work, the authors introduce the physical properties of SET and simulate current-voltage characteristics in single electron transistor by non-equilibrium Green's function method using graphic user interface (GUI) of Matlab. Here, a model of multiple level device for SET (i.e. it takes quantization into account in quantum dot) has been used. The theoretical approach based on NEGF, review the capabilities of the simulator, NEMO-VN2 [19] are also summarized with examples of typical simulations of SET's current-voltage characteristics and simulated results comparison with experimental ones.

2. BASIC PHYSICS, MODELING AND SIMULATION OF SET

The operation of a single electron tunneling device is governed by the Coulomb charging effect. As shown in Figure 1a, a single electron tunneling device consists of a nanometer-scale conductive or semiconducting

island (quantum dot) embedded in an insulating material. Electrons travel between the island, source (S) and drain (D) through thin insulating tunnel junctions. When an electron tunnels into the island, the overall electrostatic potential of the island increases by e/C_{Σ} , where e is the elementary charge and C_{Σ} is island capacitance. For large devices, this change in potential is negligible due to the high capacitance C_{Σ} . However, for nanometer-scale islands, C_{Σ} is much smaller (about aF).

Change to SET island potential results an energy gap at the Fermi energy, preventing further electron tunneling. This phenomenon is called Coulomb blockade. It prevents current from flowing between source and drain ($I_{ds} = 0$), i.e, the SET is turned off. The Coulomb blockade effect can be overcome by changing the voltage of a conductor capacitively coupled to the island, thereby turning tunneling on or off.

As shown in Figure 1 a SET typically has three terminals. The source and drain terminals serve as electron reservoirs. When the SET is turned on, electrons tunnel from one terminal, through the junction, to the conductive island. They then tunnel through the other junction to the other terminal. Each tunneling junction is modeled as resistor (R_S or R_D) and capacitor (C_S or C_D) in parallel.

A gate terminal (G), with coupling capacitance C_G , controls the transport of electrons. The Coulomb blockade effect is maximized when $V_{GS} = me/C_G$, where $m = \pm 1, \pm 2, \pm 3, \dots$ because, at these voltages, the system is in minimum-energy state when an integer number of electrons are present on the island. The Coulomb blockade effect vanishes when $m = \pm 1/2, \pm 3/2, \dots$, i.e., when m is a half-integer value because, at these voltages, the system is in a minimum-energy state when a half-integer number of electrons

are present on the island. In this case, the single tunneling event does not move the system from a minimum energy state. Electrons can therefore tunnel, in single-file, through the island as determined by V_{DS} .

In order to observe the Coulomb blockade effect, the following constraints must be satisfied.

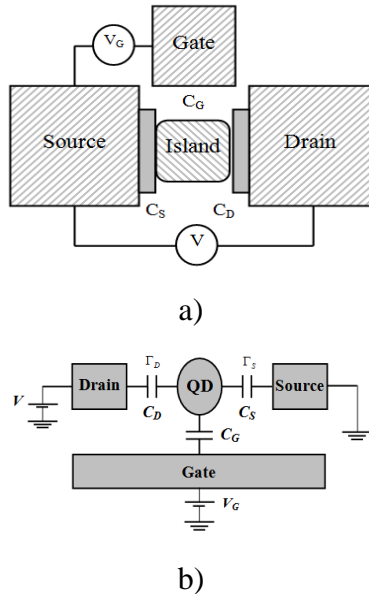


Figure 1. a) Structure of SET, b) equivalent schematic diagram of SET: C_G - gate capacitance, C_S - source tunnel junction capacitance, C_D - drain tunnel junction capacitance, R_S - source tunnel junction resistance, R_D - drain tunnel junction resistance.

(i) Since thermal fluctuations can suppress the Coulomb blockade effect, the electrostatic charging energy, e^2/C_Σ , must be much greater than $k_B T$, where k_B is Boltzmann's constant and T is the temperature. In order to ensure reliability, $e^2/C_\Sigma \geq k_B T$ other more conservative, $e^2/C_\Sigma \geq 40k_B T$ constraint is enforced. These equations imply that the maximum allowed island capacitance is inversely proportioned to temperature. At room temperature, an island capacitance

below 1 aF is required. Island capacitance is function of island size. As shown in Table 1 room temperature operation requires an island size in the nanometer range, making fabrication challenging. At present, the smallest island capacitance of a fabricated device is around 0.15 aF [9].

(ii) To observe single-electron charging effects, electrons must be confined to the island, which requires that the junction resistance be higher the quantum resistance, i.e., $R_S, R_D > h/e^2$, $h/e^2 = 25.8 \text{ k}\Omega$, where h is Plank's constant. Therefore, SETs have high resistances and low driving current.

In order to operate voltage-state logic, SETs must exhibit voltage gain. The low-temperature voltage gain is equal to the gate capacitance divided by the sum of the junction capacitances: $G = C_G/(C_S+C_D)$. Achieving this gain requires low tunneling junction capacitances. It also requires close coupling of gate and island without a large increase in the total island capacitance. High gain has only been demonstrated for a few devices and has required operation at low temperature. However, further advances in nanofabrication may overcome this limitation.

Table 1. Island size estimation. (Assuming disc capacitor model, $C_\Sigma = 8\epsilon r$. One size embedded in silicon dioxide. Other side exposed to Nitrogen).

Temperature (K)	$C_\Sigma = e^2/10k_B T$	
	Island cap. (aF)	Island diameter(nm)
40	4.65	52.48
77	2.41	27.26
103	1.80	20.38
120	1.55	17.49
200	0.93	10.50
250	0.74	8.4
300	0.62	7.0

We describe a SET's model for a multiple level device whose energy levels are described by a Hamiltonian matrix $[H]$ and whose coupling to the source and the drain contacts is described by self-energy matrices $[\Sigma_1(E)]$ and $[\Sigma_2(E)]$ respectively (Fig.2).

The flow of current is due to the difference in potentials between the source and the drain, each of which is in a state of local equilibrium, but maintained at different electro-chemical potentials $\mu_{1,2}$ and hence with two distinct Fermi functions:

$$f_1(E) = \frac{1}{\exp[(E-\mu_1)/k_B T] + 1} \quad (1)$$

$$f_2(E) = \frac{1}{\exp[(E-\mu_2)/k_B T] + 1} \quad (2)$$

by the applied bias V : $\mu_2 - \mu_1 = -qV$. Here, E - energy, k_B - Boltzmann constant, T - temperature.

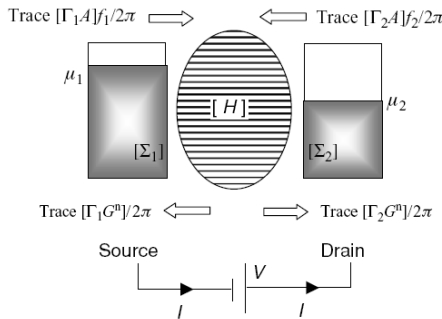


Figure 2. Multi-level device whose energy levels are described by a Hamiltonian matrix $[H]$ and whose coupling to the source and drain contacts is described by self-energy matrices $[\Sigma_1(E)]$ and $[\Sigma_2(E)]$ respectively.

The density matrix is given by

$$\rho = \int_{-\infty}^{+\infty} \frac{dE}{2\pi} G^n(E) = \int_{-\infty}^{+\infty} \frac{dE}{2\pi} [A_1(E)f_1(E) + A_2(E)f_2(E)] \quad (3)$$

The current I_D flows in the external circuit is given by Landauer formula [8]:

$$I_D = (q/h) \int_{-\infty}^{+\infty} dE T(E) (f_1(E) - f_2(E)) \quad (4)$$

The quantity $T(E)$ appearing in the current equation (4) is called the transmission function, which tells us the rate at which electrons transmit from the source to the drain contacts by propagating through the device. Knowing the device Hamiltonian $[H]$ and its coupling to the contacts described by the self-energy matrices $\Sigma_{1,2}$, we can calculate the current from (4). For coherent transport, one can calculate the transmission from the Green's function method, using the relation:

$$T(E) = \text{Trace}[\Gamma_1 G \Gamma_2 G^+] + \text{Trace}[\Gamma_2 G \Gamma_1 G^+] \quad (5)$$

The appropriate NEGF equations are obtained:

$$G = [EI - H - \Sigma_1 - \Sigma_2]^{-1},$$

$$\Gamma_{1,2} = i[\Sigma_{1,2} - \Sigma_{1,2}^+], A_1(E) = GI,$$

$$G^n = [A_1]f(E) + [A_2]f(E),$$

$$A = i[G - G^+] = [A_1] + [A_2] \quad (6)$$

Where H is effective mass Hamiltonian, I is an identity matrix of the same size, $\Gamma_{1,2}$ are the broadening functions, $A_{1,2}$ are partial spectral functions, $A(E)$ are spectral function, G^n is correlation function. We use a discrete lattice with N points spaced by lattice spacing a to calculate the eigenenergies for electrons in the quantum dot.

By utilizing the simulator namely NEMO-VN2 [26], the I_D - V_G characteristics of SET having the given parameters are shown in Figure 3.

Figure 3 demonstrates the typical Coulomb oscillation behavior in SET I_D - V_G characteristics. It shows that the SET Coulomb oscillation period (e/C_G , e is the electronic charge) is dictated by SET's gate capacitance. Values of gate voltage at the first and the second peaks are $e/2C_G$ (80mV) and $3e/2C_G$ (240mV) respectively. Here, it should be emphasized

that the peak and the valley currents of Coulomb oscillations are perfectly represented by the model. The results calculated according to model ($e/2C_G$ for $C_G = 1$ aF) coincide well with the simulated ones. Current-voltage (I_D - V_G) characteristics showing the suppression of the Coulomb oscillation by broadening current peaks increased at high V_D (200 mV). It also reveals the fact that it is difficult to obtain the Coulomb oscillations in the device characteristics at high V_D greater than $3e/C_T$ (C_T is total capacitance of SET), (160 mV). It should note that high drain voltage, V_D undermines SET's current-voltage characteristics.

Figure 4 reproduces SET's I_D - V_D characteristics at room temperature ($T = 300$ K) for different gate biases, $V_G = 0$ mV and $V_G = e/2C_G$ (Coulomb oscillation).

For $V_G = 0$ mV, V_D starts from the Coulomb blockade region and increases (or decreases) through the single-electron tunneling region. For $V_G = e/2C_G$ (at the first Coulomb oscillation peak), I_D starts from zero and increases (or decreases) linearly. The threshold voltage of SET is $V_G = e/2C_G$.

Accuracy of the model is evaluated by comparing simulated results with experimental ones from [8].

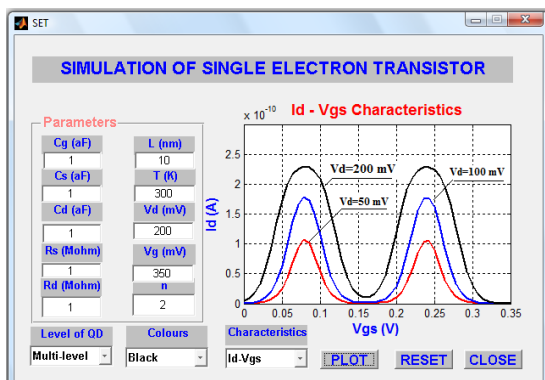


Figure 3. Typical I_D - V_G characteristics (Coulomb oscillations) of SET simulated by the simulator NEMO-VN2 for various values of $V_D = 50$ mV, 100 mV and 200 mV at room

temperature, $T = 300$ K. The SET parameters are: $L = 10$ nm, $C_G = C_S = C_D = 1$ aF and $R_S = R_D = 1$ M Ω .

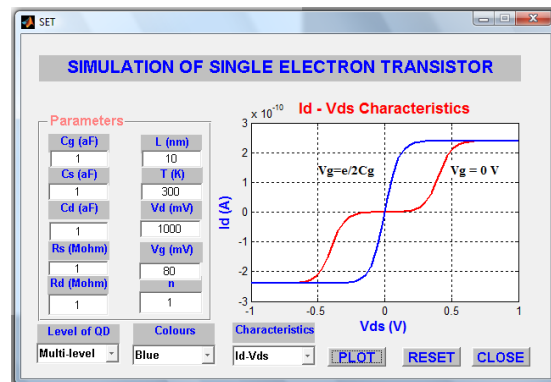


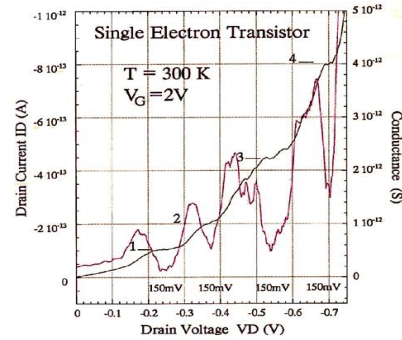
Figure 4. I_D - V_D characteristics simulated by the simulator at room temperature $T = 300$ K for various values of $V_G = 0$ mV and $V_G = e/2C_G$. The SET parameters are: $L = 10$ nm, $C_G = C_S = C_D = 1$ aF and $R_S = R_D = 1$ M Ω .

According to the work [8], its authors have succeeded in fabricating an SET. The SET operates at room temperature, showing a clear Coulomb staircase with a ~ 150 mV period at 300K. The drain current-voltage characteristics of the SET were measured at room temperature and are shown in figure 5a. The gate bias was set to 2V. In the Figure, the solid lines show the current of the SET, and the dashed line shows the conductance of the SET. Between the drain bias of 0 V and -0.75 V, four clear Coulomb staircases with a ~ 150 mV period are observed. The conductance oscillates with the increase of the drain bias with almost the same 150 mV period. The lower peaks of the conductance oscillation correspond to the flat regions of the current of the Coulomb staircase. The drain current versus gate bias characteristics with 150 mV drain bias at room temperature exhibit clear current oscillations with a period of ~ 460 mV, implying a periodic Coulomb oscillation of the current. The tunneling capacitance (C_T) and gate

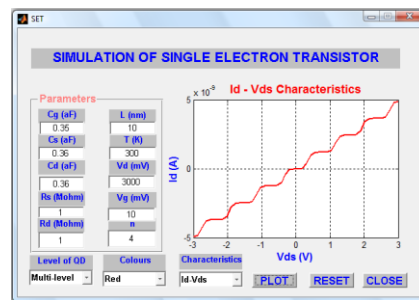
capacitance (C_g) could be roughly estimated from the period of the Coulomb staircase and oscillation. Their values were found to be $C_t = \sim 3.6 \times 10^{-19} \text{F}$ and $C_G = \sim 3.5 \times 10^{-19} \text{F}$. Fig.5b,c reproduce I_D - V_D characteristics and conductance of the same SET having length, $L = 10 \text{ nm}$ at temperature of 300 K. Figures 5b,c show simulated results of I_D - V_D characteristics and conductance of the same SET. Four clear Coulomb staircases are shown in simulated results on I_D - V_D characteristics (Fig.5b). Four clear conductance peaks are also shown in Fig.5c. The results simulated according to the model coincide well with the experimental ones at least in the same shape.

3. CONCLUSIONS

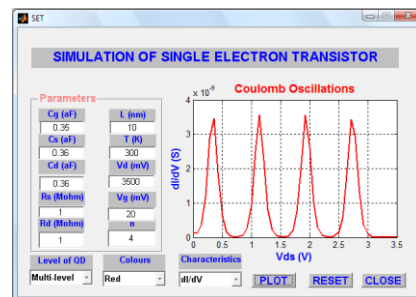
Basic physical properties, fabrication method, and the most popular simulators of SET have been introduced. A model for SET device using NEGF written in GUI of Matlab has been reported. The proposed model has been verified at multiple level for SET's device. A set of simulations is then successfully performed for various parameters of the SET's device in multi-level mode (i.e. it takes quantization into account in the quantum dot). The model is not only able to accurately describe I_D - V_G , I_D - V_D SET's characteristics, but also affects of gate materials, size of SET, temperature on SET's characteristics. Different SET's device characteristics (I_D - V_G , I_D - V_D , effect of temperature) have been simulated. The simulated results are also compared with experimental ones [8] and good agreements are validated.



a)



b)



c)

Figure 5. a) Drain current versus drain voltage characteristics of the SET at 300 K [8]: $V_D = 150 \text{ mV}$, $C_t = 0.36 \text{ aF}$, $C_G = 0.35 \text{ aF}$; b) I_D - V_D characteristics simulated; c) Conductance characteristics simulated by the simulator, NEMO-VN2 for value of $V_G = 20 \text{ mV}$. The SET device parameters are: $L = 10 \text{ nm}$, $C_G = 0.35 \text{ aF}$, $C_S = C_D = 0.36 \text{ aF}$ and $R_S = R_D = 1 \text{ M}\Omega$

REFERENCES

- [1] International technology roadmap for semiconductors, 2006, <http://public.itrs.net>.
- [2] D. V. Averin and K. K. Likharev, Coulomb blockade of tunneling and coherent oscillations in small tunnel junctions, *J. Low Temperature Physics*, 62, 345-372, 1986.

- [3] T. A. Fulton and J. G. Dolan, Observation of single electron charging effects in small tunnel junctions, *Physics Review Lett.*, 59, 109-112, 1987.
- [4] K.K. Likharev, Single electron devices and their applications, *Proc. IEEE*, 87, 606-632, 1999.
- [5] Y. Nakamura, C. D. Chen, and J. S. Tsai, 100 K operation of Al-based single electron transistors, *Japan Journal of Applied Physics*, 35, 1465-1467, 1996.
- [6] X. Tang, X. Baie, V. Bayot, F. Van de Wiele, J. P. Colinge, An SOI single electron transistor, *Proceedings of Silicon on Insulator Conference*, Oct. 1999, 46-47.
- [7] M. Ahlskog, R Tarkiainen, L. Roschier, and P. Hakonen, Single electron transistor made of two crossing multi-walled carbon nanotubes and its noise properties, *Applied Physics Lett.*, 77, 4037-4039, 2000.
- [8] K. Matsumoto, M. Ishii, K Segawa, Y. Oka, B. J. Vartanian, and J.S.Harris, Room temperature operation of a single electron transistor made by the scanning tunneling microscope nanooxidation process for the TiO/Ti system, *Appl. Phys. Lett.* 68, 34 (1996): doi:101063/1, 116747.
- [9] J. I. Shirakashi, K. Matsumoto, N. Miura, M. Kanagai, Single electron charging effects in Nb/Nb oxide-based single electron transistor at room temperature, *Applied Physics Lett.* 72, No.15, 1893-1895, 1998.
- [10] Y. A. Pashkin, Y. Nakamura, and J. S. Tsai, Room-temperature Al single electron transistor made by electron beam lithography, *Applied Physics Lett.* 76, No. 16, 2256-2258, 2000.
- [11] J. R. Heath and M. A. Ratner, Molecular electronics, *Physics Today*, vol. 56, p. 43-49, 2003.
- [12] A. K. Geim and K. S. Novoselov, The rise of grapheme, *Nature materials*, 6, 183-191, 2007.
- [13] C. Wasshuber, *Computational Electronics*, New York: Springer-Verlag, (2002).
- [14] R. H. Chen, A. N. Karotkov, and K. K. Likharev, A new logic family based on single electron transistors, *Proceedings of Device Res. Conf.*, 44-45, Charlottesville, 19-21 June 1995.
- [15] K. Uchida, R. Matsuzawa, J. Koga, R. Ohba, S. Takagi and A. Toriumi, Analytical single electron transistor (SET) model for design and analysis of realistic SET circuits, *Jpn. J. Appl. Phys.*, 39, 2321-2324, 2000.
- [16] Hiroshi Inokawa and Yamo Takashi, A compact analytical model for asymmetrical single-electron transistors, *IEEE Transactions on Electron Devices*, 50, No. 2, 455-461, 2003.
- [17] S. Mahapatra, V. Vainish, C. Wasshuber, K. Banerjee, and A. M. Ionescu, Analytical modeling of single electron transistor (SET) for hybrid CMOS-SET analog IC design, *IEEE Trans. Electron Devices*, 51, No. 11, 1772-1782, 2004.
- [18] S. Datta, *Quantum Transport: Atom to Transistor*, Cambridge University Press, (2005).
- [19] Dinh Sy Hien, Development of quantum device simulator, NEMO-VN2, *Proceedings of fifth IEEE international symposium on electronic design, test and applications*, DELTA-2010, 13-15 January 2010, Ho Chi Minh City, 170-173, 2010.

Corresponding author:

Le Hoang Minh

Ho Chi Minh City University of Technology

Email: minhhlh@hcmute.edu.vn